

Dithienocarbazole-Based Ladder-Type Heptacyclic Arenes with Silicon, Carbon, and Nitrogen Bridges: Synthesis, Molecular Properties, Field-Effect Transistors, and Photovoltaic Applications

Jhong-Sian Wu, Yen-Ju Cheng,* Tai-Yen Lin, Chih-Yu Chang, Peng-I. Shih, and Chain-Shu Hsu*

A new class of ladder-type dithienosilolo-carbazole (DTSC), dithienopyrrolo-carbazole (DTPC), and dithienocyclopenta-carbazole (DTCC) units is developed in which two outer thiophene subunits are covalently fastened to the central 2,7-carbazole cores by silicon, nitrogen, and carbon bridges, respectively. The heptacyclic multifused monomers are polymerized with the benzothiadiazole (BT) acceptor by palladium-catalyzed cross-coupling to afford three alternating donor-acceptor copolymers poly(dithienosilolo-carbazole-*alt*-benzothiadiazole) (PDTSCBT), poly(dithienocyclopenta-carbazole-*alt*-benzothiadiazole) (PDTCCBT), and poly(dithienopyrrolo-carbazole-*alt*-benzothiadiazole) (PDTPCBT). The silole units in DTSC possess electron-accepting ability that lowers the highest occupied molecular orbital (HOMO) and lowest unoccupied molecular orbital (LUMO) energy levels of PDTSCBT, whereas stronger electron-donating ability of the pyrrole moiety in DTPC increases the HOMO and LUMO energy levels of PDTPCBT. The optical bandgaps (E_g^{opt}) deduced from the absorption edges of thin film spectra are in the following order: PDTSCBT (1.83 eV) > PDTCCBT (1.64 eV) > PDTPCBT (1.50 eV). This result indicated that the donor strength of the heptacyclic arenes is in the order: DTPC > DTCC > DTSC. The devices based on PDTSCBT and PDTCCBT exhibited high hole mobilities of 0.073 and 0.110 $\text{cm}^2 \text{V}^{-1} \text{s}^{-1}$, respectively, which are among the highest performance from the OFET devices based on the amorphous donor-acceptor copolymers. The bulk heterojunction photovoltaic device using PDTSCBT as the p-type material delivered a promising efficiency of 5.2% with an enhanced open circuit voltage, V_{oc} , of 0.82 V.

1. Introduction

Research on polymer-based solar cells (PSCs) and field-effect transistors (FET) using organic p-type semiconductors have attracted tremendous scientific and industrial interest in recent

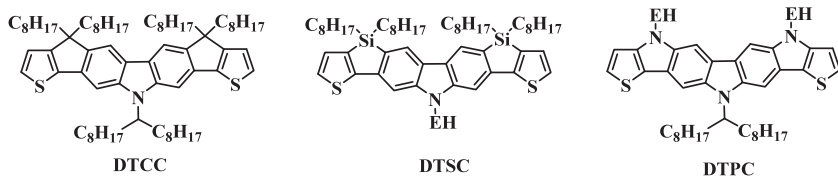
J.-S. Wu, Prof. Y.-J. Cheng, T.-Y. Lin, C.-Y. Chang,
P.-I. Shih, Prof. C.-S. Hsu
Department of Applied Chemistry
National Chiao Tung University
1001 Ta Hsueh Road Hsin-Chu, 30010, Taiwan
E-mail: yjcheng@mail.nctu.edu.tw;
cshsu@mail.nctu.edu.tw



DOI: 10.1002/adfm.201102906

years.^[1] Besides device engineering and morphology control, development of p-type conjugated polymers continues to play a pivotal role to achieve high efficiency of PSCs. Successful approaches to producing low bandgap (LBG) polymers involve the incorporation of electron-rich donor and electron-deficient acceptor segments along the conjugated polymer backbone.^[2] Planarization of polyaromatic system facilitates the π -electron delocalization and elongates the effective conjugation length, providing another effective way to reduce the optical bandgap.^[3] Moreover, coplanar geometries and rigid structures can suppress the rotational disorder around interannular single bonds and lower the reorganization energy, which in turn enhances the intrinsic charge mobility.^[4] In accordance with these guidelines, development of donors by hybridizing different aromatic or heteroaromatic units into mutually fused structure is highly promising. Consequently, ladder-type conjugated structures with forced coplanarity have gained considerable attention for applications in organic photovoltaics.^[5] At the same time, such kind of structures are also very attractive to prepare conjugated polymers for achieving high hole mobilities in polymer-based FETs.^[5c,5f,5g,6] However, realization of chemical rigidification is synthetically challenging and requires elegant molecular design. To promote sufficient solubility of highly coplanar aromatic π -system, it is necessary that bridging atom must have extra valence for introducing aliphatic side chains. In this regard, carbon (C), silicon (Si), and nitrogen (N) are the most viable bridging elements to fasten two neighboring aryl rings, thus forming cyclopentadiene, silole, and pyrrole units embedded in the multifused system. Importantly, each bridging atom possesses different steric and orbital nature, which provides a useful tool to tailor electronic and optical properties of the ladder-type conjugated system. For instance, coplanar bithiophene units, cyclopentadithiophene, (CPDT, bridged by a carbon), dithienosilole (bridged by a silicon), and dithienopyrrole (DTP, bridged

zation of chemical rigidification is synthetically challenging and requires elegant molecular design. To promote sufficient solubility of highly coplanar aromatic π -system, it is necessary that bridging atom must have extra valence for introducing aliphatic side chains. In this regard, carbon (C), silicon (Si), and nitrogen (N) are the most viable bridging elements to fasten two neighboring aryl rings, thus forming cyclopentadiene, silole, and pyrrole units embedded in the multifused system. Importantly, each bridging atom possesses different steric and orbital nature, which provides a useful tool to tailor electronic and optical properties of the ladder-type conjugated system. For instance, coplanar bithiophene units, cyclopentadithiophene, (CPDT, bridged by a carbon), dithienosilole (bridged by a silicon), and dithienopyrrole (DTP, bridged

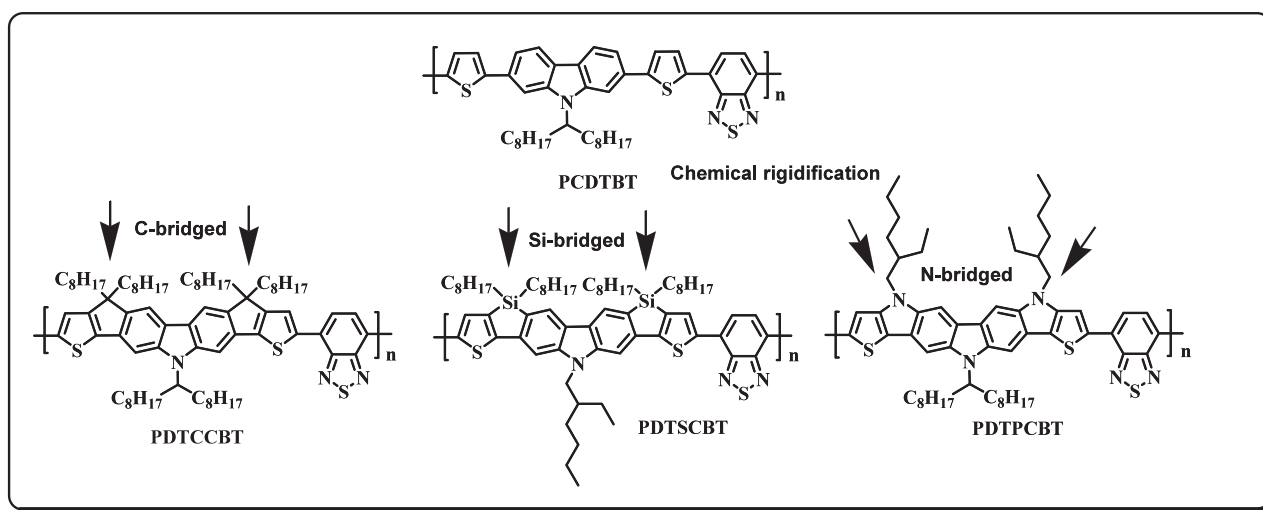


Scheme 1. C-, Si- and N-bridged heptacyclic structures, **DTCC**, **DTSC**, and **DTPC**. EH is 2-ethylhexyl.

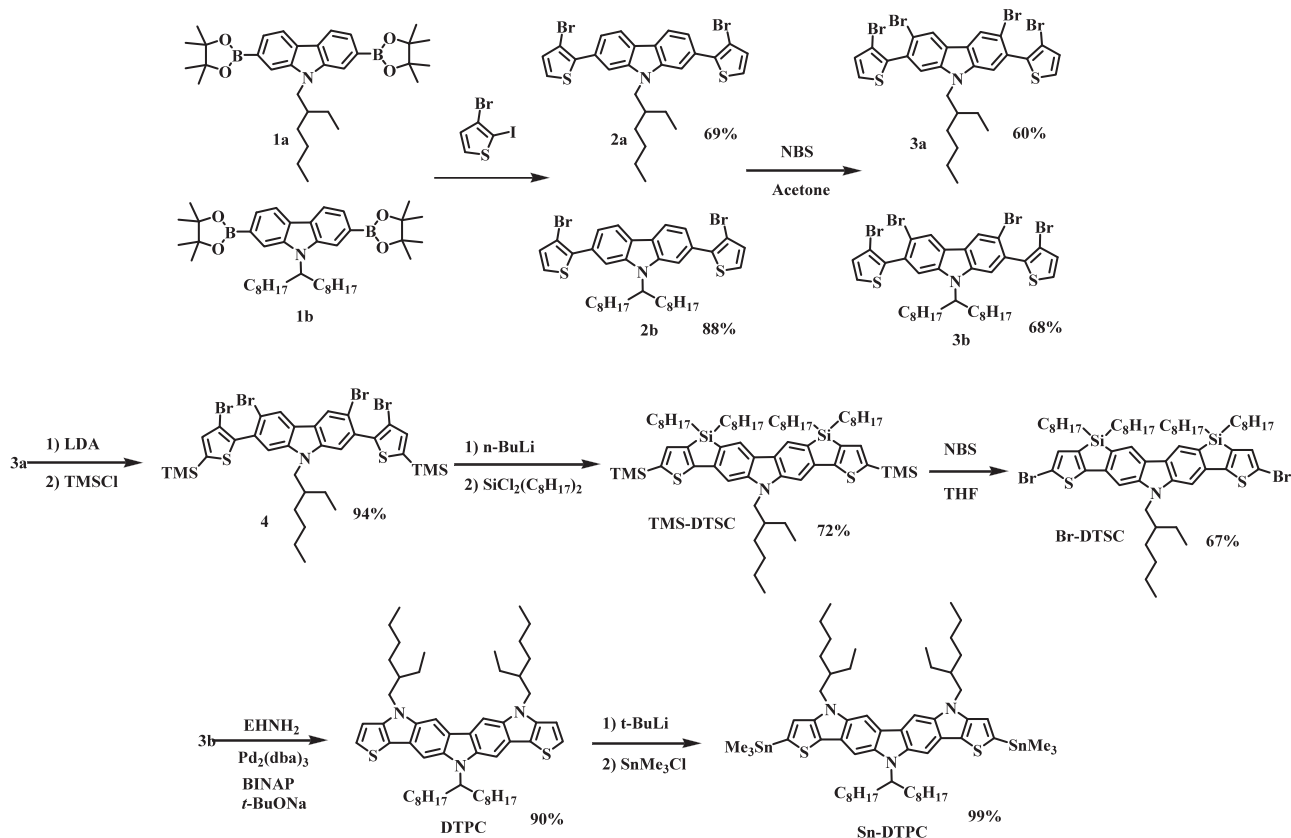
by a nitrogen) have been employed as the building blocks to make a range of donor-acceptor copolymers. **DTP**-based polymers have shown relatively narrower bandgap (≈ 1.13 to 1.59 eV) and high hole mobilities as a result of the enhanced electron-donating ability of the central pyrrole ring.^[7] Although the chemical structure of poly(cyclopentadithiophene-*alt*-benzothiadiazole) **PCP-DTBT** and poly(dithienosilole-*alt*-benzothiadiazole) **PSBTBT** is almost identical, except that the bridging C-atom in the backbone is replaced by a Si-atom, **PSBTBT** is demonstrated to have higher crystallinity and hole mobility than **PCPDTBT** due to longer C–Si bond.^[8] In fact, compared with the five-membered heterocycles such as thiophene, furan, and pyrrole, silole exhibits extraordinary molecular properties as a result of its unique $\sigma^*-\pi^*$ conjugation.^[9] Therefore, silole units are very appealing building block to construct conjugated systems for optoelectronic applications.

Tricyclic 2,7-carbazole unit is a widely used electron-rich building block to construct donor-acceptor polymers because its derivatives exhibit deep-lying highest occupied molecular orbital (HOMO) energy levels and good hole-transporting properties, which are crucial prerequisites to achieve high open-circuit voltages (V_{oc}) and short circuit currents (J_{sc}), respectively. Poly(2,7-carbazole-*alt*-dithienylbenzothiadiazole) (**PCDTBT**) has shown to be a superior p-type photoactive material for applications in PSCs (**Scheme 1**).^[10] Inspired by the repeating unit in **PCDTBT** polymer, electron-rich dithienylcarbazole motif is an ideal structural basis for designing a series of fascinating ladder-type multifused conjugated frameworks. If the 3-positions of the two outer thiophenes are covalently connected with

the 3- and 6-positions of the central carbazole core by two atomic bridges, new ladder-type coplanar heptacyclic arenes will be emerged. By utilizing Friedel–Craft cyclization, we have first successfully synthesized a sp^3 -hybridized carbon-bridged system, dithienocyclopentacarbazole (**DTCC**), which consists of two embedded cyclopentadiene (CP) rings (Scheme 1). The device incorporating the **DTCC**-based poly(dithienocyclopentacarbazole-*alt*-benzothiadiazole) (**PDTCCBT**) polymer has shown promising performance.^[5d,5e] To tailor and control the optical and electronic properties, it is highly desirable to further elaborate this system by incorporating sp^3 -hybridized silicon or nitrogen elements to replace the carbon bridges. As such, two novel heptacyclic dithienosilole-carbazole (**DTSC**) and dithienopyrrolo-carbazole (**DTPC**) structures will be present with silole and pyrrole units fused between the thiophene and carbazole units, respectively (**Scheme 2**). We envisaged that utilization of silicon or nitrogen bridges would not only planarize the skeleton but also perturb the electronic properties through orbital interactions. In this research, we disclose two facile cyclization approaches to successfully construct **DTSC** and **DTPC** heptacyclic units in good yield. On the basis of the modified **DTSC** and **DTPC** units as electron-rich donors to polymerize with the benzothiadiazole acceptor, two novel alternating donor-acceptor copolymers poly(dithienosilole-carbazole-*alt*-benzothiadiazole) (**PDTSCBT**) and poly(dithienopyrrolo-carbazole-*alt*-benzothiadiazole) (**PDTPCBT**) have been synthesized. In terms of structural uniqueness for PSCs material development, **PDTPCBT** is the first LBG polymer containing a strong electron-donating donor with three N-bridged atoms, while **PDTSCBT** is the first LBG copolymer containing three heteroatoms (sulfur, silicon, nitrogen) in a coplanar conjugated system. These ladder-type heptacyclic systems have exhibited very intriguing properties. The synthesis, characterization, molecular properties, and applications in PSCs and FETs will be discussed in detail.



Scheme 2. Chemical structure of the polymers in this research.



Scheme 3. Synthetic route for the monomers.

2. Results and Discussion

2.1. Synthesis of Monomers and Polymers

The synthetic route of the DTSC and DTPC monomers is depicted in Scheme 3. 2,7-diboronic ester carbazole (1a and 1b) were reacted with 3-bromo-2-iodothiophene by Suzuki coupling to obtain compound 2a and 2b, respectively. Due to the nitrogen-directing effect, bromination of compound 2 by 2 eq of N-bromosuccinimide (NBS) regioselectively occurs at 3- and 6-positions of the carbazole unit to obtain tetra-brominated key intermediate 3. Lithiation of compound 3a by LDA followed by quenching with trimethyl silyl chloride yielded compound 4 with two trimethyl silyl groups as the protecting groups. After metal-bromo exchange of compound 4 by using *n*-butyllithium (*n*-BuLi), the tetra-lithiated intermediate was subjected to cyclization through double nucleophilic addition of dioctyldichlorosilane. By this synthetic strategy, we are able to efficiently generate two silole rings to complete the synthesis of Si-bridged heptacyclic structure TMS-DTSC (TMS: trimethylsilyl) in good reaction yield of 72%. NBS bromination via electrophilic aromatic substitution to replace the trimethylsilyl moiety resulted in the formation of compound Br-DTSC in 67% yield.

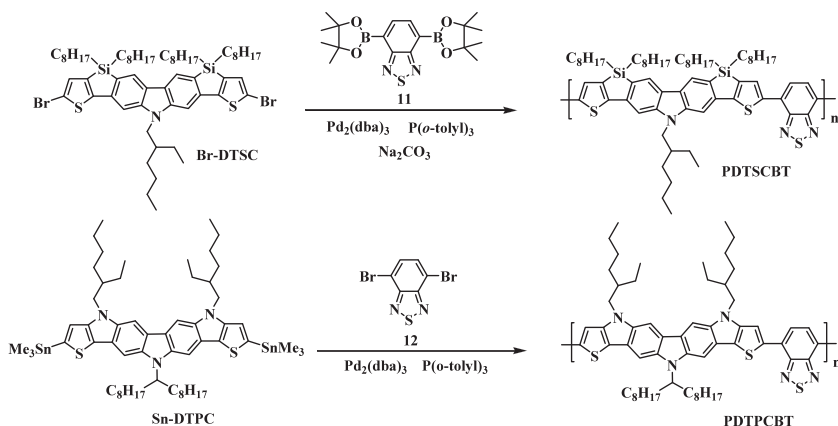
At the same time, we envision that 2,7-bis(3-bromothiophen-2-yl)-3,6-dibromo-carbazole 3b can also serve as an ideal substrate for the synthesis of N-bridged DTPC structure by palladium-catalyzed amination. Fortunately, DTPC was also

successfully synthesized by reacting 3b with 2-ethylhexylamine via Buchwald–Hartwig reaction in excellent yield of 90% in the presence of Pd₂(dba)₃ (tris(dibenzylideneacetone)dipalladium) as the catalyst and BINAP (2,2'-bis(diphenylphosphino)-1,1'-binaphthyl) as the ligand. It should be noted that using excess amount of 2-ethylhexylamine (11 eq) is the key to successfully carrying out intramolecular amination to form two pyrrole units in just one step. DTPC can be efficiently lithiated by *t*-butyllithium followed by reacting with trimethyltin chloride to afford Sn-DTPC.

Monomer Br-DTSC was copolymerized with the acceptor, 4,7-bis(4,4,5,5-tetramethyl-1,3,2-dioxaborolan-2-yl)-2,1,3-benzothiadiazole, by Suzuki coupling to give PDTSCBT, while Sn-DTPC was also copolymerized with the acceptor, 4,7-dibromo-2,1,3-benzothiadiazole, by Stille coupling to give PDTPCBT (*M_n* = 36.4 kDa, polydispersity index (PDI) = 1.21) (Scheme 4 and Table 1). The molecular weight of PDTSCBT is not obtainable from gel permeation chromatography (GPC) measurement due to its poor solubility in tetrahydrofuran (THF).

2.2. Thermal Properties

The thermal stability was analyzed by thermogravimetric analysis (TGA). PDTSCBT and PDTPCBT exhibited sufficiently high decomposition temperatures (*T_d*) of 449 °C and 402 °C, respectively, indicating that PDTSCBT is thermally more stable than PDTPCBT (Figure S1 (Supporting Information) and Table 1). Thermal



Scheme 4. Synthesis of alternating PDTSCBT and PDTPCBT polymers.

Table 1. Molecular weight and thermal properties of the polymers.

Polymer	M_n [kDa]	PDI	T_g [°C]	T_d [°C]
PDTSCBT	NA	NA	NA	449
PDTPCBT	36.4	1.21	226	402
PDTCCBT ^{a)}	38.1	1.60	139	422

^{a)}Data from ref. [4d].

properties of the polymers were determined by differential scanning calorimetry (DSC). Both polymers exhibited the amorphous nature. Besides, PDTPCBT showed a glass transition temperature (T_g) at 226 °C. (Figure S2 (Supporting Information) and Table 1).

2.3. Electrochemical Properties

To better understand the bridging atom effect on the electrochemical properties of the heptacyclic system, cyclic voltammetry

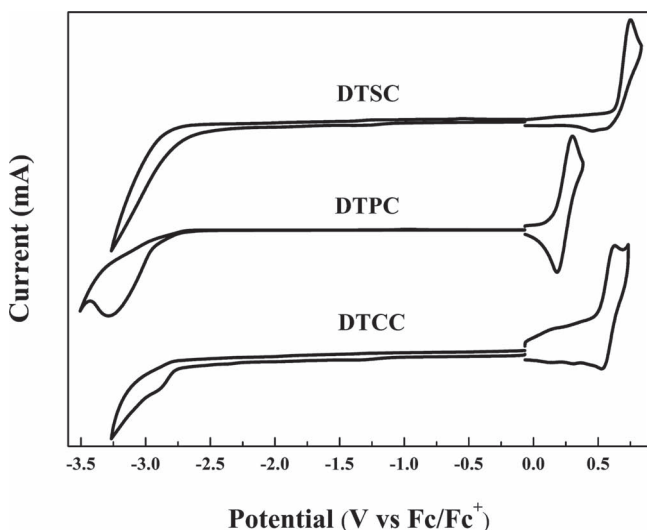


Figure 1. Cyclic voltammograms of monomers DTSC, DTPC, and DTCC in the THF solution at a scan rate of 50 mV s⁻¹.

(CV) was used to evaluate the HOMO and lowest unoccupied molecular orbital (LUMO) levels of the C-bridged DTCC, Si-bridged DTSC and N-bridged DTPC heptacyclic arenes (Figure 1) as well as their corresponding copolymers (Figure 2). The electrochemical properties are summarized in Table 2 and the energy diagram is shown in Figure 3. The HOMO/LUMO energy levels of DTPC, DTCC, and DTSC were determined to be -4.97/-1.91 eV, -5.32/-2.03 eV and -5.45/-2.19 eV with the corresponding bandgaps of 3.06, 3.29, and 3.26 eV respectively. This result indicated that the HOMO/LUMO energy levels are highly dependent on the bridging elements in the heptacyclic backbone. It is known that silole unit possesses certain extent of electron-accepting ability, which in turn lowers the HOMO/LUMO energy levels of DTSC. In contrast, the stronger electron-donating ability of the pyrrole moiety will increase the HOMO/LUMO energy levels of DTPC and the carbon atom in the cyclopentadiene ring of DTCC features more insulating character toward the π -conjugated system. After the heptacyclic monomers were copolymerized with the benzo-

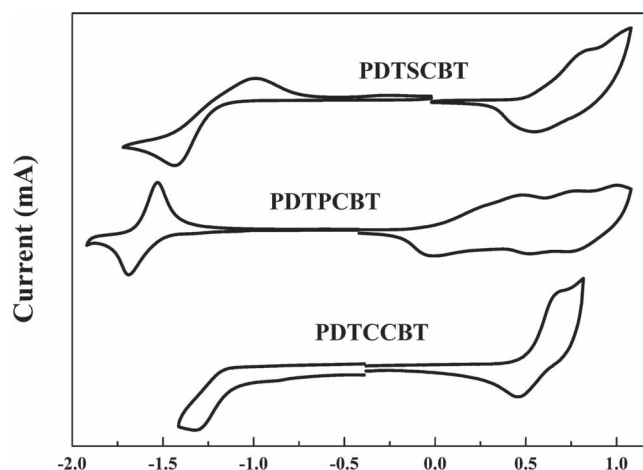


Figure 2. Cyclic voltammograms of PDTSCBT, PDTPCBT, and PDTCCBT in the thin film at a scan rate of 50 mV s⁻¹.

Table 2. Electrochemical properties of the heptacyclic arenes and polymers.

Monomer	HOMO [eV]	LUMO [eV]	E_g^{ec} [eV] ^{a)}
DTSC	-5.45	-2.19	3.26
DTPC	-4.97	-1.91	3.06
DTCC	-5.32	-2.03	3.29
PDTSCBT	-5.35	-3.58	1.77
PDTPCBT	-4.76	-3.29	1.47
PDTCCBT	-5.31	-3.67	1.64

^{a)} E_g^{ec} = electrochemical bandgap (LUMO-HOMO).

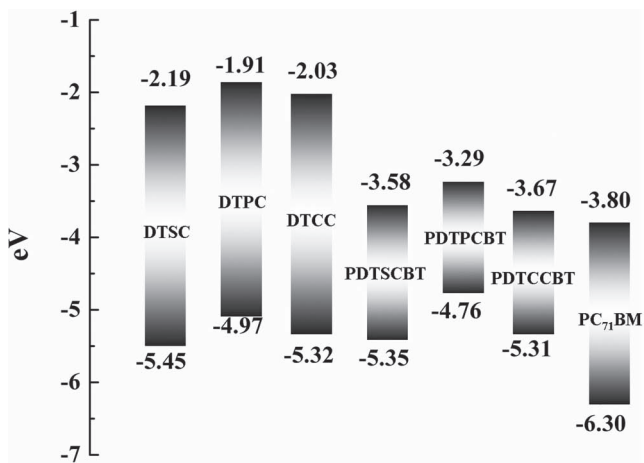


Figure 3. HOMO and LUMO energy levels of the heptacyclic arenes and polymers estimated by CV.

thiadiazole acceptor, the corresponding polymers exhibit higher HOMO energy levels and lower LUMO energy levels, leading to significantly reduced electrochemical bandgaps. The bridging atoms of the heptacyclic units still play a key role in determining the HOMO energy levels of the polymers (-4.76 , -5.31 , and -5.35 eV for **PDTPCBT**, **PDTCCBT**, and **PDTSCBT**, respectively) (Table 2). The trend of relative HOMO positions in the polymers is consistent with the trend observed in the corresponding monomers. The lowest-lying HOMO level observed for Si-bridged **PDTSCBT** may ensure better air-stability and greater attainable V_{oc} in the final device. The higher-lying HOMO level of **PDTPCBT** is due to the oxidative property of the dithienopyrrole unit in **DTPC**. The LUMO energy levels are located at -3.58 eV for **PDTSCBT** and -3.29 eV for **PDTPCBT**, which are positioned 0.2 to 0.3 eV

above the LUMO level of the **PC₇₁BM** ([6,6]-phenyl-C₇₁-butyric acid methyl ester) acceptor (-3.8 eV) to induce energetically favorable electron transfer^[11] (Figure 3).

2.4. Optical Absorption and Photoluminescence

The absorption spectra of monomers and polymers are shown in Figure 4. Note that the absorption spectra of all the heptacyclic arenes consist of several sharp peaks or shoulders with very narrow bandwidth (Figure 4a). This fine structure clearly reflects the highly rigid and coplanar feature of the conjugated structure.

The absorption maximum of the heptacyclic arenes is also associated with their bridging atoms. Compared to **DTPC** showing the absorption maximum at 390 nm in the toluene solution, **DTCC** and **DTSC** exhibited bathochromic shifts of the absorption maxima at 394 and 395 nm, respectively (Table 3). However, it was observed that N-bridge **DTPC** shows two low-energy transitions at 421 and 446 nm, which may come from the vibronic transition with lower oscillating strength. For all the polymers, the shorter wavelength absorbance comes from the $\pi-\pi^*$ transition of the heptacyclic units, while the lower energy band is attributed to the photoinduced intramolecular charge transfer (ICT) between the electron-rich and the electron-deficient benzo-thiadiazole unit. In contrast to the trend observed in the small molecules, N-bridged **PDTPCBT** exhibited the most bathochromic shift of the absorption ICT maximum at 742 nm in the toluene solution, whereas Si-bridged **PDTSCBT** exhibited the most hypsochromic shift absorption maximum at 590 nm. Furthermore, the optical bandgaps (E_g^{opt}) deduced from the absorption edges of thin film spectra are in the following order: **PDTSCBT** (1.83 eV) > **PDTCCBT** (1.64 eV) > **PDTPCBT** (1.50 eV). Note that these values are in good agreement with the bandgaps (E_g^{EC}) estimated by electrochemical measurement (**PDTSCBT** = 1.77 eV, **PDTCCBT-C8** = 1.64 eV, and **PDTPCBT** = 1.47 eV). The transition energy of the photoinduced charge transfer band is highly dependent on the donating strength of the donor and accepting strength of the acceptor in the conjugated backbone. Because all of the polymers have the same acceptor, the difference of their λ_{max} as well as E_g^{opt} indicates that the donor strength of the heptacyclic arene is in the order: **DTPC** > **DTCC** > **DTSC**. Compared to **DTCC**, the weaker electron-donating ability of **DTSC** is again associated with the electron-accepting effect of silole units. In the solid state, the polymers exhibited bathochromic shifts of the ICT band and broader absorption bands compared to the spectra obtained in toluene, indicating stronger $\pi-\pi$ stacking formed in the thin film.

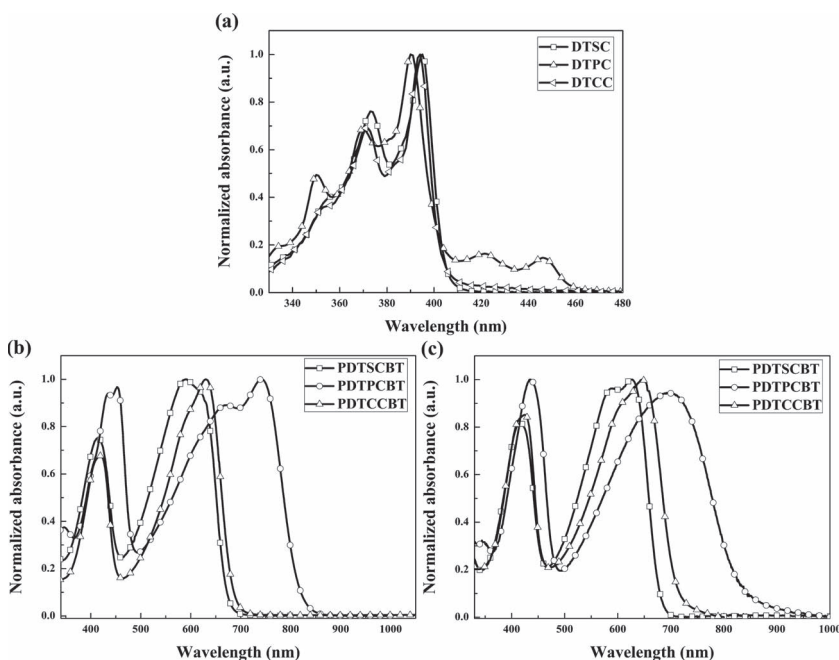


Figure 4. Normalized absorption spectra of: a) **DTSC**, **DTPC** and **DTCC** in toluene solution; b) **PDTPCBT**, **PDTCCBT**, and **PDTSCBT** in toluene solution; and c) the solid state.

The emission spectra of the monomers and copolymers are also investigated and shown in Figure 5. In the heptacyclic arenes, compared to **DTSC** and **DTCC** showing very similar emission profiles in the toluene solution, **DTPC** exhibited the much bathochromic-shifted spectrum with maximum emission at 484 nm

Table 3. Optical Properties of the Heptaarenes and Copolymers.

Monomer and Polymer	Absorption λ_{\max} [nm]		E_g^{opt} (Film) [eV]	Emission λ_{\max} in toluene [nm]	Stokes Shift [cm^{-1}]
	Toluene	Film			
DTSC	395	–	3.07 ^{a)}	424	1731
DTPC	390	–	2.71 ^{a)}	484	4980
DTCC	394	–	3.09 ^{a)}	426	1906
PDTSCBT	415, 590	416, 626	1.83 ^{b)}	689	9583
PDTPCBT	453, 742	435, 702	1.50 ^{b)}	834	10085
PDTCCBT	419, 630	425, 645	1.64 ^{b)}	716	9900

^{a)} E_g^{opt} from the onset of UV spectra in toluene solution; ^{b)} E_g^{opt} from the onset of UV spectra in thin film.

(Table 3). On the other hand, the λ_{\max} of emission spectra in toluene are located at 689 nm, 716 nm, and 834 nm for PDTSCBT, PDTCCBT, and PDTPCBT, respectively, which is consistent with the trend of λ_{\max} in their corresponding absorption spectra (i.e., 590 nm for PDTSCBT < 630 nm for PDTCCBT < 742 nm for PDTPCBT in toluene). All the polymers showed large Stokes shift deduced from the difference between the absorption and emission maxima in the solution. PDTPCBT exhibited the largest Stokes shift (10 085 cm^{-1}) followed by PDTCCBT (9900 cm^{-1}) and

PDTSCBT (9583 cm^{-1}). This result again suggests that PDTPCBT has strongest donor-acceptor charge transfer character upon excitation, whereas PDTSCBT has the lowest.

2.5. Theoretical Calculations

To gain more insight into the molecular orbital properties of the heptacycles and the polyaromatic π -electron systems, theoretical calculations were performed with time-dependent density functional theory (TD-DFT) at the level of B3LYP/6-311G(d,p) (Table 4); solvent effect (in toluene) was included by the polarizable continuum model.^[12] Considering a minimal effect on electronic properties, all the side-chain substituents were replaced with methyl groups

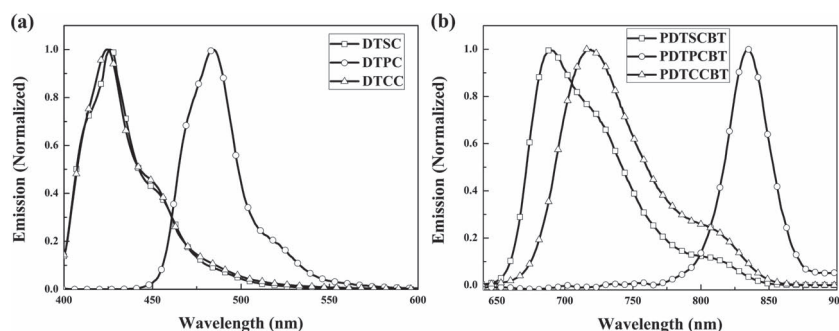



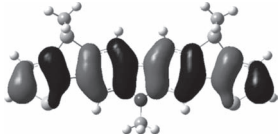
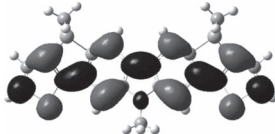
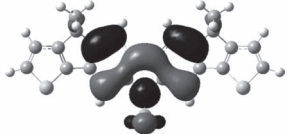
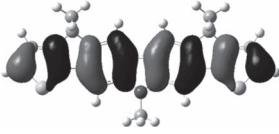
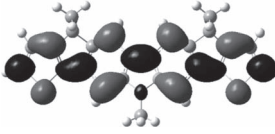
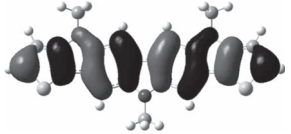

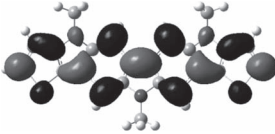
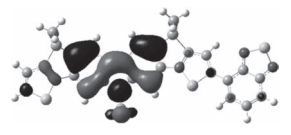
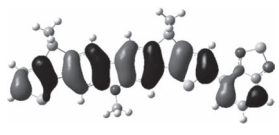
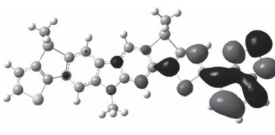
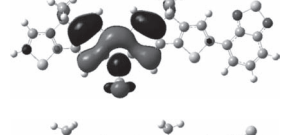
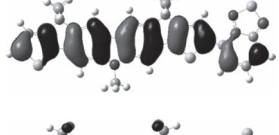
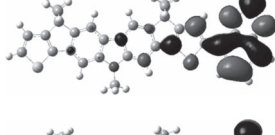
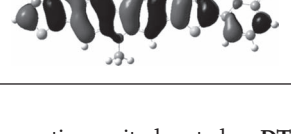
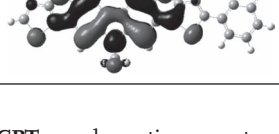
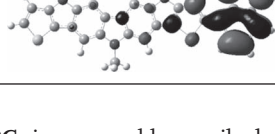
Figure 5. Normalized emission spectra of a) DTSC, DTPC, and DTCC and b) PDTSCBT, PDTPCBT, and PDTCCBT in toluene solution.

Table 4. Calculated (TD-B3LYP/6-311G(d,p), PCM = toluene) HOMO/LUMO energy, excitation energy, oscillator strength, and configurations (with large CI coefficients) of the excited state.

Compound	HOMO [eV]	LUMO [eV]	Excitation energy		Oscillator strength	Configuration ^{a)}
			$\lambda_{\max, \text{exp}}$ [nm]	λ_{calc} [nm]		
DTSC	−5.24	−1.70	395	395.87	1.32	H → L
				364.43	0.03	H−1 → L
						H → L+1
						H → L+2
DTPC	−4.99	−1.43	≈450	428.74	0.07	H → L
				390	390.04	1.29
DTCC	−5.13	−1.58	394	392.37	1.46	H → L
				365.19	0.04	H−1 → L
						H → L+2
PDTSCBT	−5.21	−2.69	415, 590	573.07	0.68	H → L
				453.52	0.01	H−1 → L
PDTPCBT	−4.98	−2.68	453, 742	665.48	0.04	H−1 → L
						H → L
				625.10	0.59	H−1 → L
PDTCCBT	−5.10	−2.70	419, 630	598.49	0.69	H → L
				478.66	0.01	H−1 → L

^{a)}Configurations with largest coefficients in the CI expansion of each excited state are highlighted in boldface.

Table 5. Plots of frontier orbitals of the heptacyclic arenes and model compounds calculated at the level of B3LYP/6-311G(d,p) in toluene.

Compound	HOMO-1	HOMO	LUMO
DTSC			
DTCC			
DTPC			
DTSCBT			
DTCCBT			
DTPCBT			

for simplicity. One repeating unit, denoted as **DTSCBT**, **DTPCBT**, and **DTCCBT**, in the more stable anti conformations were used as simplified model compounds for the simulation of **PDTSCBT**, **PDTPCBT**, and **PDTCCBT**, respectively. Visualization of HOMO (H), LUMO (L), and the closely HOMO-1 (H-1) is shown in **Table 5**. The HOMO and LUMO energies are directly taken from the DFT calculations (**Table 5** and **Figure 6**). Although there are variations in the absolute values, satisfactory correlations between the molecular orbital (MO) energies from TD-DFT and electrochemical experiments were found. Si-bridged **DTSC** and **DTSCBT** exhibit the lowest-lying HOMO energy levels compared to their C- and N-bridged counterparts. For the three heptacycles, the energies of the most probable vertical excitations for **DTSC**, **DTPC**, and **DTCC** are calculated to be 396, 390, and 392 nm, respectively, which are in good agreement with their λ_{max} in absorption spectra. These strong absorptions are assigned to H \rightarrow L transitions for **DTSC** and **DTCC**, and H-1 \rightarrow L for N-bridged **DTPC**. It should be noted that the orbital electron distribution of HOMO for **DTSC** and **DTCC** are very similar to that of HOMO-1 for **DTPC**. On the other hand, the orbital pattern of HOMO for **DTPC** resembles to that of HOMO-1 for **DTSC** and **DTCC**, except that stronger orbital coefficient was found on N bridging atom in the HOMO of **DTPC**. No orbital coefficient is located at Si and C bridges in the HOMO-1 of **DTSC** and **DTCC**. As a result, a weak characteristic peak at low-energy of 421 nm observed in the

absorption spectrum of **DTPC** is reasonably ascribed to the H \rightarrow L transition with a small oscillator strength ($f < 0.1$, $\lambda_{\text{calc.}} = 428$ nm). Similarly, for the models of polymers, the energies of the strongest transitions for **DTSCBT**, **DTCCBT**, and **DTPCBT** are calculated to be 573 nm (H \rightarrow L), 598 nm (H \rightarrow L), and 625 nm (H-1 \rightarrow L), respectively. The frontier orbitals of the model compounds were also shown in **Table 5**. The same orbital characters can also be observed among the **DTSCBT**, **DTPCBT**, and **DTCCBT**. The electron densities of the HOMO for **DTSCBT** and **DTCCBT**, and HOMO-1 for **DTPCBT** are homogeneously distributed along the heptacyclic donor units, while the electron density of the LUMO energy levels is redistributed to the BT acceptor unit. Such an electronic redistribution suggests a pronounced intramolecular charge separation in the copolymers after excitation.

2.6. Characteristics of Organic Field-Effect Transistors

Considering the coplanar geometries and rigid structures of the heptacyclic arenes, it is highly desirable to utilize these polymers for application in organic FETs (OFETs). The hole mobilities of solution-processed **PDTSCBT**, **PDTPCBT**, and **PDTCCBT** thin film were measured using a bottom-gate, top-contact device configuration with evaporated gold source/drain electrodes and octadecyltrichlorosilane-modified SiO₂ gate dielectric on n-doped

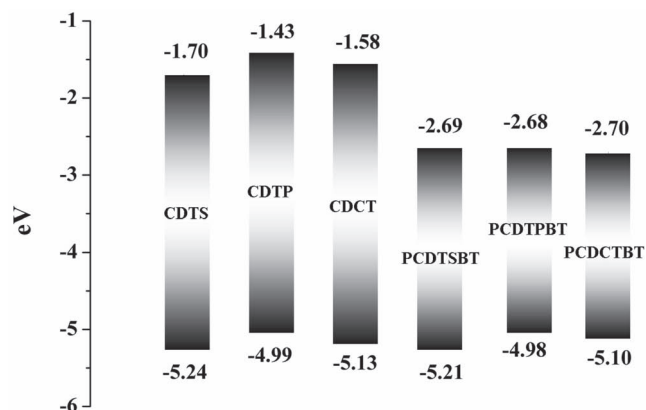


Figure 6. Theoretical HOMO and LUMO energy levels of the heptacycles and model compounds for the polymers.

silicon wafer surface. The output and transfer plots (at the same source-drain voltages of -60 V) of the devices exhibited typical p-channel OFET characteristics (**Figure 7**). The hole mobilities were obtained from the transfer characteristics of the devices

in saturation regime. The thin film of PDTPCBT was annealed at 200 °C for 10 min under nitrogen, annealed PDTPCBT device showed the hole mobility of 8.5×10^{-4} $\text{cm}^2 \text{V}^{-1} \text{s}^{-1}$ with an on-off ratio of 4.0×10^2 (**Table 6**). Encouragingly, the devices of PDTSCBT and PDTCCBT exhibited higher hole mobilities of 0.073 and 0.110 with good on-off ratios of 1.1×10^6 and 1.7×10^4 in the optimal condition (120 °C for 10 min), respectively (**Table 6**). After thermal treatments, all of the polymers showed their highest hole mobility due to the enhanced intermolecular stacking. To our knowledge, the hole mobilities of PDTSCBT and PDTCCBT are among the best performances in the amorphous benzothiadiazole-based donor-acceptor type copolymers. It is envisaged that DTSC and DTCC copolymerized with thieno[3,2-b]thiophene units might show higher hole mobilities because of thieno[3,2-b]thiophene have been used extensively in many copolymers with high charge carrier mobilities.^[13]

2.7. Photovoltaic Characteristics

Bulk heterojunction photovoltaic cells were fabricated by spin-coating the blends from ortho-dichlorobenzene (ODCB)

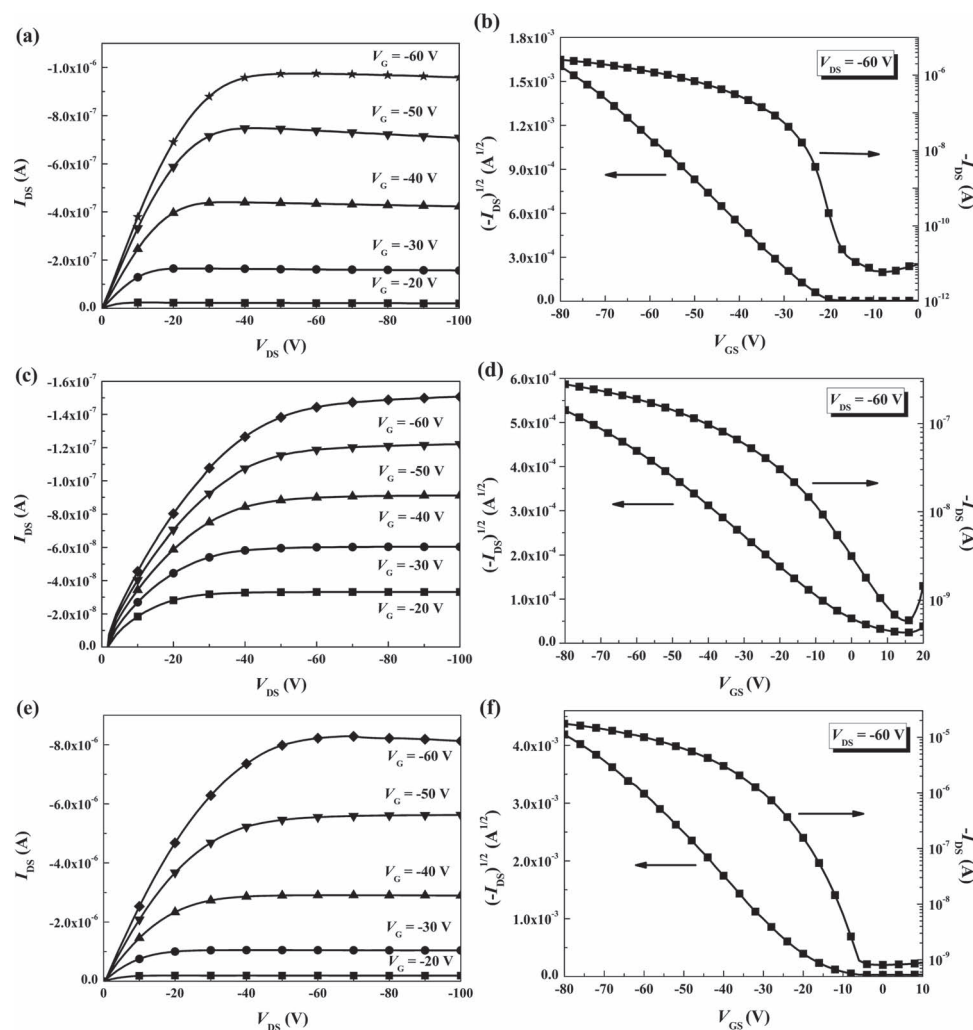


Figure 7. Typical output curves (a,c,e) and transfer plots (b,d,f) of the OFET devices based on PDTSCBT, PDTPCBT, and PDTCCBT, respectively.

Table 6. Device characteristics.

Polymer	Blend ratio with PC ₇₁ BM	$\mu_{\text{h}}^{\text{a}}$ [cm ² V ⁻¹ s ⁻¹]	V_{oc} [V]	J_{sc} [mA cm ⁻²]	FF [%]	PCE [%]
PDTSCBT	1:3	≈0.063 to 0.073	0.82	11.1	56.7	5.2
PDTPCBT	1:2	≈6.1 to 8.5×10^{-4}	0.50	10.5	49.9	2.6
PDTCCBT ^{b)}	1:3	≈0.084 to 0.110	0.74	10.3	60.0	4.6

^{a)}Hole mobility of the polymers determined by OFET; ^{b)} Device data from ref. [4d].

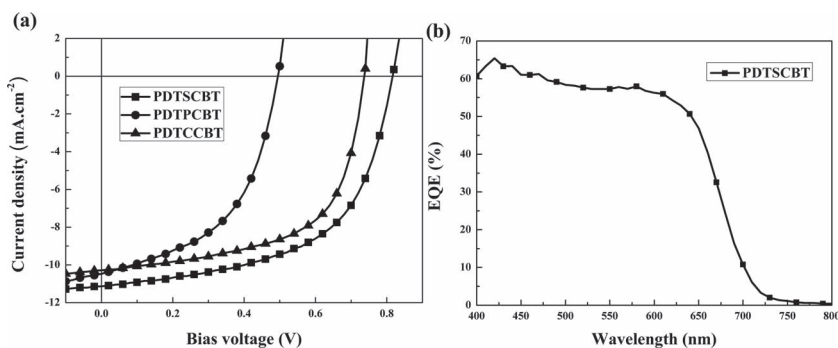


Figure 8. a) Current density–voltage characteristics and b) EQE spectrum of ITO/PEDOT:PSS/polymer:PC₇₁BM/Ca/Al devices under illumination of AM 1.5 G at 100 mW cm⁻².

solutions at various polymer-to-PC₇₁BM ratios on the basis of indium tin oxide (ITO)/poly(3,4-ethylenedioxythiophene):poly(styrenesulfonate) (PEDOT:PSS)/polymer:PC₇₁BM/Ca/Al configuration and their performances were measured under a simulated AM 1.5 G illumination of 100 mW cm⁻². The current density–voltage characteristics of the devices are shown in Figure 8a. The blend ratio of the active layers shown in the Table 6 is the result of the optimized conditions for the devices. The device based on the PDTPCBT:PC₇₁BM (1:2 in wt%) blend exhibited a V_{oc} of 0.50 V, a J_{sc} of 10.5 mA cm⁻², a fill factor (FF) of 49.9%, delivering an power conversion efficiency (PCE) of 2.6%. Encouragingly, the device using PDTSCBT:PC₇₁BM (1:3 in wt%) as the p-type material delivered a superior performance with a V_{oc} of 0.82 V, a J_{sc} of 11.1 mA cm⁻², a FF of 56.7%, improving the PCE to 5.2%. The V_{oc} values of the devices are plotted as a function of HOMO energy levels of the corresponding polymers in Figure 9, showing a proportional relationship. Compared to PDTPCBT and PDTCCBT, the largest V_{oc} of the PDTSCBT-based device is associated with the lowest-lying HOMO of Si-bridged PDTSCBT. The incident photon to current efficiency (IPCE) spectra of PDTSCBT exhibits over EQE of 55% in the range of 400–620 nm (Figure 8b).

3. Conclusions

A new class of heptacyclic ladder-type arenes based on dithienylcarbazole skeleton is developed. The 3-positions of the two outer thiophenes are covalently connected with the 3- and 6-positions of the central carbazole core by silicon, carbon and nitrogen bridges, respectively, creating dithienosilolocarbazole (DTSC), dithienocyclopenta-carbazole (DTCC), and

dithienopyrrolo-carbazole (DTPC) structures. Facile lithiation/silylation and Pd-catalyzed amination of 2,7-bis(3-bromothiophen-2-yl)-3,6-dibromo-carbazole successfully construct the silole units in DTSC and the pyrrole units in DTPC, respectively, in good yield. The ladder-type monomers were further polymerized with the benzothiadiazole acceptor to furnish three alternating donor-acceptor copolymers PDTSCBT, PDTCCBT, and PDTPCBT. Utilization of silicon or nitrogen bridges not only planarizes the backbone but also perturbs the orbital interactions. The silole units in DTSC possess certain extent of electron-accepting ability which

lowers the HOMO/LUMO energy levels of PDTSCBT, whereas the stronger electron-donating ability of the pyrrole moiety in DTPC increases the HOMO/LUMO energy levels of PDTPCBT. The optical bandgaps ($E_{\text{g}}^{\text{opt}}$) deduced from the absorption edges of thin film spectra are in the following order: PDTSCBT (1.83 eV) > PDTCCBT (1.64 eV) > PDTPCBT (1.50 eV), indicating that the donor strength of the heptacyclic arene is in the order: DTPC > DTCC > DTSC. The FET device based on PDTPCBT exhibited a hole mobility of 8.5×10^{-4} cm² V⁻¹ s⁻¹ with an on-off ratio of 4.0×10^2 . Moreover, the devices based on PDTSCBT and PDTCCBT exhibited higher hole mobilities of 0.073 and 0.110 cm² V⁻¹ s⁻¹, respectively. These mobili-

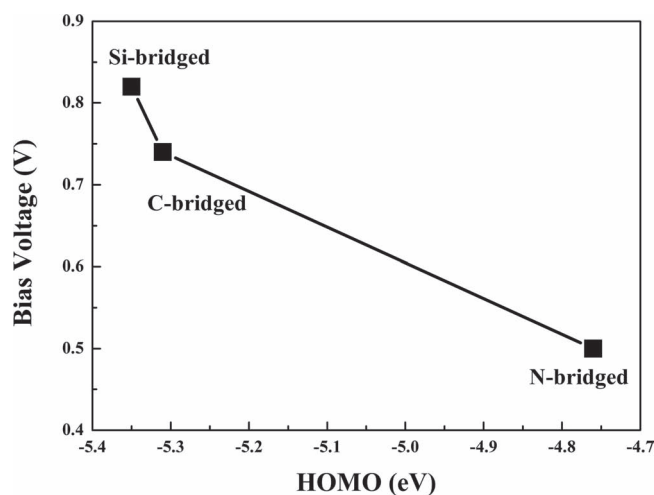


Figure 9. The relation between V_{oc} and the HOMO of the corresponding copolymers.

ties are among the best performance from the amorphous donor-acceptor copolymers. The bulk heterojunction device using Si-bridged PDTSCBT as the p-type material delivered the best efficiency PCE to 5.2% with a V_{oc} of 0.82 V, a J_{sc} of 11.1 mA cm⁻², a FF of 56.7%. The embedded silole units to effectively lower the HOMO energy level of PDTSCBT are responsible for the highest V_{oc} value of the device.

4. Experimental Section

General Measurement and Characterization: All chemicals were purchased from Aldrich or Acros and used as received unless otherwise specified. ¹H and ¹³C NMR spectra were measured using a Varian 300 MHz instrument spectrometer. Fourier transform infrared (FTIR) spectra were on a Perkin-Elmer One Instrument by preparing KBr Pellets. Differential scanning calorimetry (DSC) was measured on a TA Q200 Instrument and thermogravimetric analysis (TGA) was recorded on a Perkin Elmer Pyris under nitrogen atmosphere at a heating rate of 10 °C min⁻¹. Absorption spectra were collected on a HP8453 UV-vis spectrophotometer. The molecular weight of polymers were measured by the GPC method on a Viscotek VE2001GPC, and polystyrene was used as the standard (THF as the eluent). The electrochemical cyclic voltammetry (CV) was conducted on a CH Instruments Model 611D. A carbon glass coated with a thin polymer film was used as the working electrode and Ag/Ag⁺ electrode as the reference electrode, while 0.1 M tetrabutylammonium hexafluorophosphate (Bu₄NPF₆) in acetonitrile was the electrolyte. CV curves were calibrated using ferrocene as the standard, whose oxidation potential is set at -4.8 eV with respect to zero vacuum level. The HOMO energy levels were obtained from the equation HOMO = -(E_{ox}^{onset} - E_(ferrocene)^{onset} + 4.8) eV. The LUMO levels of polymer were obtained from the equation LUMO = -(E_{red}^{onset} - E_(ferrocene)^{onset} + 4.8) eV.

Synthesis of 2-Ethylhexyl-2,7-bis(3-bromo-2-thienyl)-9H-carbazole (2a): 2,7-Bis(4',4',5',5'-tetramethyl-1',3',2'-dioxaborolan-2'-yl)-N-9"-2-ethylhexylcarbazole **1a**^[14] (5.88 g, 11.07 mmol), 3-bromo-2-iodothiophene^[15] (7.67 g, 26.55 mmol), K₂CO₃ (9.18 g, 66.42 mmol), Aliquant 336 (1.12 g, 2.77 mmol), and Pd(PPh₃)₄ (1.28 g, 1.11 mmol) were dissolved in deoxygenated toluene/H₂O (78 mL, 5:1, v/v). The reaction mixture was refluxed at 120 °C for 72 h and then extracted with diethyl ether (100 mL × 3) and water (150 mL). The collected organic layer was dried over MgSO₄. After removal of the solvent under reduced pressure, the residue was purified by column chromatography on silica gel (hexane/dichloromethane, v/v, 20/1) to give a pale yellow sticky product **2a** (4.56 g, 69%). ¹H NMR (CDCl₃, 300 MHz, ppm): δ 0.85 (t, J = 7.2 Hz, 3 H), 0.95 (t, J = 7.2 Hz, 3 H), 1.25-1.45 (m, 8 H), 2.10-2.17 (m, 1 H), 4.21 (d, J = 7.5 Hz, 2 H), 7.11 (d, J = 5.4 Hz, 2 H), 7.33 (d, J = 5.4 Hz, 2 H), 7.49 (dd, J₁ = 8.1 Hz, J₂ = 1.2 Hz, 2 H), 7.76 (d, J = 1.2 Hz, 2 H), 8.12 (d, J = 8.1 Hz, 2 H); MS (EI, C₂₈H₂₇Br₂NS₂): calcd, 601.46; found, 601.

Synthesis of Compound 3a: N-bromosuccinimide (1.24 g, 6.97 mmol) was added in one portion to a solution of **2a** (2.0 g, 3.33 mmol) in acetone (60 mL). The reaction was stirred under dark for 12 h at room temperature. The mixture solution was extracted with diethyl ether (150 mL × 3) and water (100 mL). The combined organic layer was dried over MgSO₄. After removal of the solvent under reduced pressure, the residue was purified by column chromatography on silica gel (hexane/dichloromethane, v/v, 15/1) to give a white solid **3a** (1.5 g, 60%). ¹H NMR (CDCl₃, 300 MHz, ppm): δ 0.80 (t, J = 7.2 Hz, 3 H), 0.89 (t, J = 7.2 Hz, 3 H), 1.20-1.40 (m, 8 H), 2.00-2.04 (m, 1 H), 4.12 (d, J = 7.5 Hz, 2 H), 7.11 (d, J = 5.4 Hz, 2 H), 7.41-7.43 (m, 4 H), 8.34 (s, 2 H); ¹³C NMR (CDCl₃, 75 MHz, ppm): δ 10.98, 14.10, 23.10, 24.32, 28.62, 30.97, 39.35, 47.95, 111.54, 113.62, 114.80, 123.57, 124.82, 126.28, 130.25, 131.35, 138.14, 140.36; IR (KBr) 3083, 2954, 2926, 2868, 2851, 1741, 1622, 1595, 1530, 1448, 1402, 1340, 1269, 1237, 1188, 1149, 1040, 871, 849, 709, 572, 513 cm⁻¹; MS (FAB, C₂₈H₂₅Br₄NS₂): calcd, 795.25; found, 795; elemental analysis (%) Calcd, for C₂₈H₂₅Br₄NS₂: C, 44.29; H, 3.32; N, 1.84. Found: C, 44.60; H, 3.53; N, 2.08.

Synthesis of Compound 4: A 2.0 M solution of lithium diisopropylamide (LDA) in hexane (1.5 mL, 3.0 mmol) was added dropwise to a solution of **3a** (1.03 g, 1.36 mmol) in dry THF (20 mL) at -78 °C. After stirring at -78 °C for 1 h, chlorotrimethylsilane (0.44 g, 4.05 mmol) was introduced by syringe to the solution. The mixture solution was warmed up to room temperature and stirred for 15 h. The mixture solution was quenched with water and extracted with diethyl ether (50 mL × 3) and water (50 mL). The combined organic layer was dried over MgSO₄. After removal of the solvent under reduced pressure, the residue was purified by column chromatography on silica gel (hexane/dichloromethane, v/v, 30/1) to give a white solid **4** (1.15 g, 94%). ¹H NMR (CDCl₃, 300 MHz, ppm): δ 0.37 (s, 18 H), 0.79 (t, J = 7.2 Hz, 3 H), 0.88 (t, J = 7.2 Hz, 3 H), 1.19-1.39 (m, 8 H), 2.02 (br, 1 H), 4.10 (d, J = 7.5 Hz, 2 H), 7.19 (s, 2 H), 7.40 (s, 2 H), 8.34 (s, 2 H); ¹³C NMR (CDCl₃, 75 MHz, ppm): δ -0.10, 11.02, 14.13, 23.13, 24.35, 28.60, 30.92, 39.29, 47.98, 112.56, 113.36, 114.51, 123.48, 124.76, 131.70, 136.42, 140.36, 141.64, 143.00; IR (KBr) 2956, 2927, 2857, 1627, 1596, 1479, 1449, 1403, 1279, 1250, 1184, 1016, 993, 843, 818, 756, 645, 622, 540 cm⁻¹; MS (FAB, C₃₄H₄₁Br₄NS₂Si₂): calcd, 903.61; found, 904; elemental analysis (%) Calcd, for C₃₄H₄₁Br₄NS₂Si₂: C, 45.19; H, 4.57; N, 1.55. Found: C, 46.53; H, 4.88; N, 1.92.

Synthesis of TMS-DTSC: The compound was synthesized by following a previously reported procedure.^[5] A 2.5 M solution of n-BuLi in hexane (2.7 mL, 6.75 mmol) was added dropwise to a solution of **4** (1.15 g, 1.27 mmol) in dry THF (30 mL) at -78 °C. After stirring at -78 °C for 1 h, the cooling bath was removed and the mixture solution was stirred at room temperature for 1 h. Subsequently, dichlorodioctylsilane (1.28 g, 3.95 mmol) was added at -78 °C. After stirring at -78 °C for 0.5 h, the mixture solution was stirred at room temperature for 14 h. The mixture solution was quenched with water and extracted with diethyl ether (60 mL × 3) and water (60 mL). The combined organic layer was dried over MgSO₄. After removal of the solvent under reduced pressure, the residue was purified by column chromatography on silica gel (hexane) to give a pale yellow sticky product **TMS-DTSC** (1.0 g, 72%). ¹H NMR (CDCl₃, 300 MHz, ppm): δ 0.37 (s, 18 H), 0.82-0.98 (m, 26 H), 1.21-1.50 (m, 56 H), 2.09 (br, 1 H), 4.10-4.22 (m, 2 H), 7.23 (s, 2 H), 7.43 (s, 2 H), 8.14 (s, 2 H).

Synthesis of Compound Br-DTSC: N-Bromosuccinimide (0.30 g, 1.69 mmol) was added in one portion to a solution of **TMS-CDTS** (0.84 g, 0.77 mmol) in THF (37 mL). The reaction was stirred under dark for 12 h at room temperature. The mixture solution was extracted with diethyl ether (60 mL × 3) and water (60 mL). The combined organic layer was dried over MgSO₄. After removal of the solvent under reduced pressure, the residue was purified by column chromatography on silica gel (hexane) to give a yellow solid **Br-DTSC** (0.57 g, 67%). ¹H NMR (CDCl₃, 300 MHz, ppm): δ 0.82-0.98 (m, 26 H), 1.20-1.43 (m, 56 H), 2.06-2.10 (m, 1 H), 4.10-4.21 (m, 2 H), 7.08 (s, 2 H), 7.28 (s, 2 H), 8.13 (s, 2 H); ¹³C NMR (CDCl₃, 75 MHz, ppm): δ 11.11, 12.71, 14.24, 22.79, 23.19, 24.23, 24.60, 28.81, 29.27, 29.37, 29.86, 30.99, 31.99, 33.47, 39.58, 47.34, 101.97, 112.03, 121.94, 124.85, 128.10, 132.58, 141.28, 141.35, 142.88, 158.04; IR (KBr) 2955, 2922, 2852, 1638, 1615, 1591, 1466, 1439, 1376, 1281, 1192, 1152, 1074, 1018, 973, 886, 835, 749, 713, 688, 671, 617, 488 cm⁻¹; MS (FAB, C₆₀H₉₁Br₂NS₂Si₂): calcd, 1106.48; found, 1106; elemental analysis (%) Calcd, for C₆₀H₉₁Br₂NS₂Si₂: C, 65.13; H, 8.29; N, 1.27. Found: C, 65.29; H, 8.23; N, 1.50.

Synthesis of N-Heptadecanyl-2,7-bis(3-bromo-2-thienyl)-9H-carbazole (2b): 2,7-Bis(4',4',5',5'-tetramethyl-1',3',2'-dioxaborolan-2'-yl)-N-9"-hepta-decylcarbazole **1b**^[10a] (0.30 g, 0.47 mmol), 3-bromo-2-iodothiophene^[15] (0.32 g, 1.11 mmol), K₂CO₃ (0.39 g, 2.82 mmol), Aliquant 336 (0.05 g, 0.12 mmol), and Pd(PPh₃)₄ (54 mg, 0.047 mmol) were dissolved in deoxygenated toluene/H₂O (12 mL, 5:1, v/v). The reaction mixture was refluxed at 120 °C for 72 h and then extracted with diethyl ether (50 mL × 3) and water (50 mL). The collected organic layer was dried over MgSO₄. After removal of the solvent under reduced pressure, the residue was purified by column chromatography on silica gel (hexane/ethyl acetate, v/v, 30/1) to give a pale yellow sticky product **2b** (0.30 g, 88%). ¹H NMR (CDCl₃, 300 MHz, ppm): δ 0.77-0.90 (m, 6 H), 1.02-1.25 (m, 24 H), 1.89-1.98 (m, 2 H), 2.28-2.39 (m, 2 H), 4.58-4.64 (m, 1 H), 7.11 (d, J = 5.4 Hz, 2 H), 7.31 (d, J = 5.4 Hz, 2 H), 7.45 (dd, J₁ = 8.1 Hz, J₂ = 1.2 Hz, 2 H),

7.76 (br, 1 H), 7.97 (br, 1 H), 8.11 (br, 2 H); ^{13}C NMR (CDCl_3 , 75 MHz, ppm): δ 14.20, 22.73, 26.96, 29.30, 29.47, 29.53, 31.89, 33.99, 56.79, 107.43, 109.77, 112.23, 120.29, 120.42, 120.69, 122.16, 123.54, 125.04, 129.87, 130.45, 131.91, 139.11, 139.54, 142.59, 158.01 (multiple carbon peaks result from phenomenon of atropisomerism^[10a]); IR (KBr) 3107, 2951, 2924, 2852, 1618, 1600, 1563, 1457, 1440, 1345, 1331, 1244, 1199, 1145, 866, 800, 705, 649, 504 cm^{-1} ; MS (FAB, $\text{C}_{37}\text{H}_{45}\text{Br}_2\text{NS}_2$): calcd, 727.70; found, 728.

Synthesis of Compound 3b: *N*-Bromosuccinimide (0.38 g, 2.12 mmol) was added in one portion to a solution of **2b** (0.67 g, 0.92 mmol) in acetone (15 mL). The reaction was stirred under dark for 12 h at room temperature. The mixture solution was extracted with diethyl ether (50 mL \times 3) and water (50 mL). The combined organic layer was dried over MgSO_4 . After removal of the solvent under reduced pressure, the residue was purified by column chromatography on silica gel (hexane) to give a pale yellow sticky product **3b** (0.55 g, 68%). ^1H NMR (CDCl_3 , 300 MHz, ppm): δ 0.79–0.90 (m, 6 H), 0.95–1.25 (m, 24 H), 1.82–1.90 (m, 2 H), 2.17–2.28 (m, 2 H), 4.44–4.51 (m, 1 H), 7.11 (d, $J = 5.4$ Hz, 2 H), 7.43 (d, $J = 5.4$ Hz, 2 H), 7.46 (br, 1 H), 7.62 (br, 1 H), 8.35 (d, $J = 6.9$ Hz, 2 H); ^{13}C NMR (CDCl_3 , 75 MHz, ppm): δ 14.21, 15.42, 22.73, 26.77, 29.24, 29.39, 29.41, 31.86, 33.75, 57.17, 65.99, 111.48, 113.59, 114.59, 115.98, 123.23, 124.62, 124.93, 126.27, 130.18, 130.80, 131.35, 138.04, 138.22, 141.55 (multiple carbon peaks result from phenomenon of atropisomerism^[10a]); IR (KBr) 3106, 2924, 2852, 1735, 1619, 1593, 1551, 1527, 1451, 1402, 1376, 1342, 1244, 1189, 1148, 1044, 867, 850, 706, 574, 517 cm^{-1} ; MS (FAB, $\text{C}_{37}\text{H}_{43}\text{Br}_4\text{NS}_2$): calcd, 885.49; found, 886; elemental analysis (%) Calcd, for $\text{C}_{37}\text{H}_{43}\text{Br}_4\text{NS}_2$: C, 50.19; H, 4.89; N, 1.58. Found: C, 50.32; H, 4.92; N, 1.52.

Synthesis of Compound DTPC: **3b** (0.32 g, 0.36 mmol), sodium *t*-butoxide (0.31 g, 3.23 mmol), tris(dibenzylideneacetone) dipalladium (67 mg, 0.073 mmol), 2,2'-bis(diphenylphosphino)-1,1'-binaphthyl (0.18 g, 0.29 mmol), and 2-ethylhexylamine (0.52 g, 4.02 mmol) were dissolved in deoxygenated toluene (15 mL). The reaction mixture was refluxed at 125 °C for 18 h and then extracted with diethyl ether (50 mL \times 3) and water (50 mL). The collected organic layer was dried over MgSO_4 . After removal of the solvent under reduced pressure, the residue was purified by column chromatography on silica gel (hexane/dichloromethane, v/v, 20/1) to give a yellow solid **DTPC** (0.27 g, 90%). ^1H NMR (acetone- d_6 , 300 MHz, ppm): δ 0.70–0.74 (m, 6 H), 0.83–0.91 (m, 6 H), 0.95–1.00 (m, 6 H), 1.08–1.39 (m, 28 H), 1.40–1.53 (m, 12 H), 1.96–2.00 (m, 2 H), 2.18–2.22 (m, 2 H), 2.50–2.61 (m, 2 H), 4.35 (d, $J = 7.5$ Hz, 4 H), 4.84–4.91 (m, 1 H), 7.26 (d, $J = 5.1$ Hz, 2 H), 7.51 (d, $J = 5.1$ Hz, 2 H), 7.81 (br, 1 H), 7.93 (br, 1 H), 8.26 (d, $J = 13.2$ Hz, 2 H); ^{13}C NMR (acetone- d_6 , 75 MHz, ppm): δ 11.17, 14.28, 14.39, 23.20, 23.76, 24.90, 27.37, 27.56, 31.45, 32.47, 33.87, 40.57, 45.38, 50.20, 56.88, 97.28, 99.83, 100.78, 101.22, 112.02, 115.67, 121.36, 122.03, 122.31, 122.72, 127.07, 136.11, 138.02, 140.37, 147.82 (multiple carbon peaks result from phenomenon of atropisomerism^[10a]); IR (KBr) 3108, 2954, 2924, 2852, 1691, 1624, 1514, 1498, 1459, 1350, 1263, 1216, 1151, 1124, 1078, 945, 831, 815, 707, 646, 485 cm^{-1} ; MS (FAB, $\text{C}_{53}\text{H}_{77}\text{N}_3\text{S}_2$): calcd, 820.33; found, 820; elemental analysis (%) Calcd, for $\text{C}_{53}\text{H}_{77}\text{N}_3\text{S}_2$: C, 77.60; H, 9.46; N, 5.12. Found: C, 77.74; H, 9.38; N, 4.99.

Synthesis of Compound Sn-DTPC: A 1.6 M solution of *t*-BuLi in hexane (1.1 mL, 1.76 mmol) was added dropwise to a solution of **CDTP** (0.47 g, 0.57 mmol) in dry THF (20 mL) at -78 °C. After stirring at -78 °C for 1 h, 1.0 M solution of chlorotrimethylstannane in THF (2.3 mL, 2.3 mmol) was introduced by syringe to the solution. The mixture solution was warmed up to room temperature and stirred for 12 h. The mixture solution was quenched with water and extracted with diethyl ether (50 mL \times 3) and water (50 mL). After removal of the solvent under reduced pressure, compound **Sn-DTPC** was obtained as yellow solid (0.65 g, 99%). ^1H NMR (acetone- d_6 , 300 MHz, ppm): δ 0.44 (s, 18 H), 0.70–0.75 (m, 6 H), 0.85–0.96 (m, 12 H), 1.02–1.30 (m, 28 H), 1.38–1.41 (m, 12 H), 1.83 (br, 2 H), 2.18–2.22 (m, 2 H), 2.41–2.44 (m, 2 H), 4.27 (d, $J = 6.9$ Hz, 4 H), 4.67 (br, 1 H), 7.31 (s, 2 H), 7.75 (br, 1 H), 7.86 (br, 1 H), 8.23 (d, $J = 12.6$ Hz, 2 H); IR (KBr) 2956, 2924, 2853, 1620, 1503, 1459, 1367, 1345, 1262, 1213, 1152, 1123, 1079, 987, 828, 802, 768, 722, 708, 531, 512 cm^{-1} ; MS (FAB, $\text{C}_{59}\text{H}_{93}\text{N}_3\text{S}_2\text{Sn}_2$): calcd, 1145.94; found, 1146.

Synthesis of PDTSCBT: Br-DTSC (0.43 g, 0.389 mmol), **11** (0.151 g, 0.389 mmol), tris(dibenzylideneacetone) dipalladium (14.2 mg, 0.016 mmol), tri(2-methylphenyl)phosphine (37.9 mg, 0.125 mmol) and Aliquant336 (two drop) were dissolved in deoxygenated toluene/ $\text{Na}_2\text{CO}_3(\text{aq})$ (24 mL, 5:1, v/v). The mixture was degassed by bubbling argon for 10 min at room temperature. The reaction mixture was refluxed at 90 °C for 30 min. The solution was dropwise added into methanol/ H_2O (200 mL, 3:1, v/v). The precipitate was collected by filtration and washed by Soxhlet extraction with acetone (12 h), hexane (12 h) and THF (24 h) sequentially. The product was re-dissolved in hot *o*-DCB (100 mL). The Pd-thiol gel (Silicycle Inc.) was added to above *o*-DCB solution to remove the residual Pd catalyst at 130 °C for 1 h. After filtration of the solution, the polymer solution was added into methanol to re-precipitate. The purified polymer was collected by filtration and dried under vacuum for 1 day to give a purplish black solid (240 mg, yield 57%).

Synthesis of PDTPCBT: Sn-DTPC (0.4 g, 0.349 mmol), **12** (0.103 g, 0.349 mmol), tris(dibenzylideneacetone) dipalladium (12.8 mg, 0.014 mmol), tri(2-methylphenyl)phosphine (34.0 mg, 0.112 mmol) and deoxygenated chlorobenzene (10 mL) were introduced to a 50 mL round bottom flask. The mixture was then degassed by bubbling nitrogen for 10 min at room temperature. The round bottom flask was placed into the microwave reactor and reacted at 180 °C for 50 min under 270 Watt. The solution was added into methanol dropwise. The precipitate was collected by filtration and washed by Soxhlet extraction with methanol (12 h), acetone (24 h), and hexane (24 h) sequentially. The product was re-dissolved in THF. The Pd-thiol gel (Silicycle Inc.) was added to above THF solution to remove the residual Pd catalyst. After filtration and removal of the solvent, the polymer was re-dissolved in THF again and added into methanol to re-precipitate. The purified polymer was collected by filtration and dried under vacuum for 1 day to give a black solid (180 mg, yield 54%, $M_n = 36.4$ kDa, PDI = 1.21). ^1H NMR (CDCl_3 , 300 MHz, ppm): δ 0.71–1.55 (m, 54 H), 2.01 (br, 8 H), 2.51 (br, 2 H), 4.25 (br, 4 H), 4.68 (br, 1 H), 7.05 (br, 2 H), 7.38–7.51 (br, 4 H), 8.31 (br, 2 H); IR (KBr) 3029, 2951, 2919, 2850, 1620, 1570, 1514, 1490, 1457, 1417, 1345, 1246, 1202, 1145, 1119, 985, 853, 819, 720, 524 cm^{-1} .

OFET Fabrication: An *n*-type heavily doped Si wafer with a SiO_2 layer of 300 nm and a capacitance of 11 nF cm^{-2} was used as the gate electrode and dielectric layer. Thin films (40–60 nm in thickness) of polymers were deposited on octadecyltrichlorosilane (ODTS)-treated SiO_2/Si substrates by spin-coating their *o*-dichlorobenzene solutions (1 mg mL^{-1}). Then, the thin films were annealed at different temperature (30, 120, or 200 °C) for 10 min. Gold source and drain contacts (30 nm in thickness) were deposited by vacuum evaporation on the organic layer through a shadow mask, affording a bottom-gate, top-contact device configuration. Electrical measurements of OTFT devices were carried out at room temperature in air using a 4156C, Agilent Technologies. The field-effect mobility was calculated in the saturation regime by using the equation $I_{\text{DS}} = (\mu W C_i / 2L) (V_G - V_T)^2$, where I_{DS} is the drain-source current, μ is the field-effect mobility, W is the channel width (500 μm), L is the channel length (50 μm), C_i is the capacitance per unit area of the gate dielectric layer, and V_G is the gate voltage.

Device Fabrication: ITO/glass substrates were ultrasonically cleaned sequentially in detergent, water, acetone, and isopropanol (IPA). The cleaned substrates were covered by a 30 nm thick layer of PEDOT:PSS (Clevios P provided by Stark) by spin coating. After annealing in a glove box at 150 °C for 30 min, the samples were cooled to room temperature. Polymers were dissolved in *o*-DCB and PC_{71}BM (purchased from Nano-C) was added. The solution was then heated at 80 °C and stirred overnight at the same temperature. Prior to deposition, the solution was filtered (1 μm filters). The solution of polymer: PC_{71}BM was then spin coated to form the active layer (90 nm). **PDTSCBT** films except **PDTPCBT** was thermally annealed at 150 °C for 10 min. The cathode made of calcium (350 nm thick) and aluminum (1000 nm thick) was sequentially evaporated through a shadow mask under high vacuum ($< 10^{-6}$ Torr). Each sample consisted of four independent pixels defined by an active area of 0.04 cm^2 . Finally, the devices were encapsulated and characterized in air.

ACKNOWLEDGEMENTS

The authors thank the National Science Council and the "ATU Program" of the Ministry of Education, Taiwan, for financial support. They also thank Yi-Lin Wu for the help of theoretical calculations.

Received: November 30, 2011

Published online: February 15, 2012

- [1] a) A. C. Arias, J. D. MacKenzie, I. McCulloch, J. Rivnay, A. Salleo, *Chem. Rev.* **2010**, *110*, 3; b) G. Yu, J. Gao, J. C. Hummelen, F. Wudl, A. J. Heeger, *Science* **1995**, *270*, 1789; c) S. Günes, H. Neugebauer, N. S. Sariciftci, *Chem. Rev.* **2007**, *107*, 1324; d) B. C. Thompson, J. M. J. Fréchet, *Angew. Chem. Int. Ed.* **2008**, *47*, 58; e) Y.-J. Cheng, S.-H. Yang, C.-S. Hsu, *Chem. Rev.* **2009**, *109*, 5868; f) J. Chen, Y. Cao, *Acc. Chem. Res.* **2009**, *42*, 1709.
- [2] a) J. Roncali, *Chem. Rev.* **1997**, *97*, 173; b) Y. Li, Y. Zou, *Adv. Mater.* **2008**, *20*, 2952.
- [3] a) J. Roncali, *Macromol. Rapid Commun.* **2007**, *28*, 1761; b) M. Forster, K. O. Annan, U. Scherf, *Macromolecules* **1999**, *32*, 3159; c) Z. Zhu, D. Waller, R. Gaudiana, M. Morana, D. Mühlbacher, M. Scharber, C. Brabec, *Macromolecules* **2007**, *40*, 1981; d) J. Jacob, S. Sax, T. Piok, E. J. W. List, A. C. Grimdale, K. Müllen, *J. Am. Chem. Soc.* **2004**, *126*, 6987; e) A. K. Mishra, M. Graf, F. Grasse, J. Jacob, E. J. W. List, K. Müllen, *Chem. Mater.* **2006**, *18*, 2879; f) S. A. Patil, U. Scherf, A. Kadashchuk, *Adv. Funct. Mater.* **2003**, *13*, 609; g) T. Freund, U. Scherf, K. Müllen, *Angew. Chem. Int. Ed.* **1995**, *33*, 2424; h) T. Freund, K. Müllen, U. Scherf, *Macromolecules* **1995**, *28*, 547; i) U. Scherf, *J. Mater. Chem.* **1999**, *9*, 1853.
- [4] a) J. L. Brédas, J. P. Calbert, D. A. da Silva Filho, J. Cornil, *Proc. Natl. Acad. Sci. USA* **2002**, *99*, 5804; b) S. Ando, J.-I. Nishida, H. Tada, Y. Inoue, S. Tokito, Y. Yamashita, *J. Am. Chem. Soc.* **2005**, *127*, 5336; c) N.-S. Baek, S. K. Hau, H.-L. Yip, O. Acton, K.-S. Chen, A. K.-Y. Jen, *Chem. Mater.* **2008**, *20*, 5734; d) Y. Liang, Y. Wu, D. Feng, S.-T. Tsai, H.-J. Son, G. Li, L. Yu, *J. Am. Chem. Soc.* **2009**, *131*, 56; e) S. Shinamura, I. Osaka, E. Miyazaki, A. Nakao, M. Yamagishi, J. Takeya, K. Takimiya, *J. Am. Chem. Soc.* **2011**, *133*, 5024.
- [5] a) F. He, W. Wang, W. Chen, T. Xu, S. B. Darling, J. Strzalka, Y. Liu, L. Yu, *J. Am. Chem. Soc.* **2011**, *133*, 3284; b) C.-P. Chen, S.-H. Chan, T.-C. Chao, C. Ting, B.-T. Ko, *J. Am. Chem. Soc.* **2008**, *130*, 12828; c) Y. Zhang, J. Zou, H.-L. Yip, K.-S. Chen, D. F. Zeigler, Y. Sun, A. K.-Y. Jen, *Chem. Mater.* **2011**, *23*, 2289; d) Y.-J. Cheng, J.-S. Wu, P.-I. Shih, C.-Y. Chang, P.-C. Jwo, W.-S. Kao, C.-S. Hsu, *Chem. Mater.* **2011**, *23*, 2361; e) J.-S. Wu, Y.-J. Cheng, M. Dubosc, C.-H. Hsieh, C.-Y. Chang, C.-S. Hsu, *Chem. Commun.* **2010**, *46*, 3259; f) J.-Y. Wang, S. K. Hau, H.-L. Yip, J. A. Davies, K.-S. Chen, Y. Zhang, Y. Sun, A. K.-Y. Jen, *Chem. Mater.* **2011**, *23*, 765; g) R. S. Ashraf, Z. Chen, D. S. Leem, H. Bronstein, W. Zhang, B. Schroeder, Y. Geerts, J. Smith, S. Watkins, T. D. Anthopoulos, H. Sirringhaus, J. C. de Mello, M. Heeney, I. McCulloch, *Chem. Mater.* **2011**, *23*, 768; h) C. H. Chen, Y.-J. Cheng, M. Dubosc, C.-H. Hsieh, C.-C. Chu, C.-S. Hsu, *Chem. Asian J.* **2010**, *5*, 2480; i) M. Zhang, X. Guo, X. Wang, H. Wang, Y. Li, *Chem. Mater.* **2011**, *23*, 4264; j) M. Forster, K. O. Annan, U. Scherf, *Macromolecules* **1999**, *32*, 3159.
- [6] a) W. Zhang, J. Smith, S. E. Watkins, R. Gysel, M. McGehee, A. Salleo, J. Kirkpatrick, S. Ashraf, T. Anthopoulos, M. Heeney, I. McCulloch, *J. Am. Chem. Soc.* **2010**, *132*, 11437; b) H. Usta, A. Facchetti, T. J. Marks, *J. Am. Chem. Soc.* **2008**, *130*, 8580; c) I. Osaka, T. Abe, S. Shinamura, E. Miyazaki, K. Takimiya, *J. Am. Chem. Soc.* **2010**, *132*, 5000; d) I. Osaka, T. Abe, S. Shinamura, K. Takimiya, *J. Am. Chem. Soc.* **2011**, *133*, 6852; e) K. Takimiya, S. Shinamura, I. Osaka, E. Miyazaki, *Adv. Mater.* **2011**, *23*, 4347.
- [7] a) Y. Zhang, J. Zou, H.-L. Yip, Y. Sun, J. A. Davies, K.-S. Chen, O. Acton, A. K.-Y. Jen, *J. Mater. Chem.* **2011**, *21*, 3895; b) W. Yue, Y. Zhao, S. Shao, H. Tian, Z. Xie, Y. Geng, *J. Mater. Chem.* **2009**, *19*, 2199; c) E. Zhou, M. Nakamura, T. Nishizawa, Y. Zhang, Q. Wei, K. Tajima, C. Yang, K. Hashimoto, *Macromolecules* **2008**, *41*, 8302; d) E. Zhou, Q. Wei, S. Yamakawa, Y. Zhang, K. Tajima, C. Yang, K. Hashimoto, *Macromolecules* **2010**, *43*, 821; e) W. Zhang, J. Li, L. Zou, B. Zhang, J. Qin, Z. Lu, Y. F. Poon, M. B. Chan-Park, C. M. Li, *Macromolecules* **2008**, *41*, 8953.
- [8] a) J. Hou, H.-Y. Chen, S. Zhang, G. Li, Y. Yang, *J. Am. Chem. Soc.* **2008**, *130*, 16144; b) M. C. Scharber, M. Koppe, J. Gao, F. Cordella, M. A. Loi, P. Denk, M. Morana, H.-J. Egelhaaf, K. Forberich, G. Dennler, R. Gaudiana, D. Waller, Z. Zhu, X. Shi, C. Brabec, *J. Adv. Mater.* **2010**, *22*, 367.
- [9] a) S. Yamaguchi, K. Tamao, *Bull. Chem. Soc. Jpn.* **1996**, *69*, 2327; b) K. Tamao, M. Uchida, T. Izumizawa, K. Furukawa, S. Yamaguchi, *J. Am. Chem. Soc.* **1996**, *118*, 11974; c) K. Tamao, S. Ohno, S. Yamaguchi, *Chem. Commun.* **1996**, 1873.
- [10] a) N. Blouin, A. Michaud, M. Leclerc, *Adv. Mater.* **2007**, *19*, 2295; b) S. Wakim, S. Beaupré, N. Blouin, B.-R. Aich, S. Rodman, R. Gaudiana, Y. Tao, M. Leclerc, *J. Mater. Chem.* **2009**, *19*, 5351; c) T.-Y. Chu, S. Alem, P. G. Verly, S. Wakim, J. Lu, Y. Tao, S. Beaupré, M. Leclerc, F. Bélanger, D. Désilets, S. Rodman, D. Waller, R. Gaudiana, *Appl. Phys. Lett.* **2009**, *95*, 063304; d) S. H. Park, A. Roy, S. Beaupré, S. Cho, N. Coates, J. S. Moon, D. Moses, M. Leclerc, K. Lee, A. J. Heeger, *Nat. Photonics* **2009**, *3*, 297; e) N. Blouin, A. Michaud, D. Gendron, S. Wakim, E. Blair, R. Neagu-Plesu, M. Belletête, G. Durocher, Y. Tao, M. Leclerc, *J. Am. Chem. Soc.* **2008**, *130*, 732; f) N. Leclerc, A. Michaud, K. Sirois, J. F. Morin, M. Leclerc, *Adv. Funct. Mater.* **2006**, *16*, 1694; g) G. Barbarella, L. Favaretto, G. Sotgiu, M. Zambianchi, C. Arbizzani, A. Bongini, M. Mastragostino, *Chem. Mater.* **1999**, *11*, 2533; h) J. Lu, F. Liang, N. Drolet, J. Ding, Y. Tao, R. Movileanu, *Chem. Commun.* **2008**, 5315; i) R. Qin, W. Li, C. Li, C. Du, C. Veit, H.-F. Schleiermacher, M. Andersson, Z. Bo, Z. Liu, O. Inganäs, U. Wurfel, F. Zhang, *J. Am. Chem. Soc.* **2009**, *131*, 14612; j) D. H. Wang, D. Y. Kim, K. W. Choi, J. H. Seo, S. H. Im, J. H. Park, O. O. Park, A. J. Heeger, *Angew. Chem. Int. Ed.* **2011**, *50*, 5519.
- [11] J. M. Halls, J. Cornil, D. A. dos Santos, R. Silbey, D.-H. Hwang, A. B. Holmes, J. L. Brédas, R. H. Friend, *Phys. Rev. B: Condens. Matter Mater. Phys.* **1999**, *60*, 5721.
- [12] M. J. Frisch, G. W. Trucks, H. B. Schlegel, G. E. Scuseria, M. A. Robb, J. R. Cheeseman, G. Scalmani, V. Barone, B. Mennucci, G. A. Petersson, H. Nakatsuji, M. Caricato, X. Li, H. P. Hratchian, A. F. Izmaylov, J. Bloino, G. Zheng, J. L. Sonnenberg, M. Hada, M. Ehara, K. Toyota, R. Fukuda, J. Hasegawa, M. Ishida, T. Nakajima, Y. Honda, O. Kitao, H. Nakai, T. Vreven, J. A. Montgomery Jr., J. E. Peralta, F. Ogliaro, M. Bearpark, J. J. Heyd, E. Brothers, K. N. Kudin, V. N. Staroverov, R. Kobayashi, J. Normand, K. Raghavachari, A. Rendell, J. C. Burant, S. S. Iyengar, J. Tomasi, M. Cossi, N. Rega, N. J. Millam, M. Klene, J. E. Knox, J. B. Cross, V. Bakken, C. Adamo, J. Jaramillo, R. Gomperts, R. E. Stratmann, O. Yazyev, A. J. Austin, R. Cammi, C. Pomelli, J. W. Ochterski, R. L. Martin, K. Morokuma, V. G. Zakrzewski, G. A. Voth, P. Salvador, J. J. Dannenberg, S. Dapprich, A. D. Daniels, Ö. Farkas, J. B. Foresman, J. V. Ortiz, J. Cioslowski, D. J. Fox, Gaussian, *Gaussian 09*, Revision A.0.2; Gaussian, Inc., Wallingford CT, **2009**.
- [13] a) H. Bronstein, Z. Chen, R. S. Ashraf, W. Zhang, J. Du, J. R. Durrant, P. S. Tuladhar, K. Song, S. E. Watkins, Y. Geerts, M. M. Wienk, R. A. Janssen, T. Anthopoulos, H. Sirringhaus, M. Heeney, I. McCulloch, *J. Am. Chem. Soc.* **2011**, *133*, 3272; b) I. McCulloch, M. Heeney, C. Bailey, K. Genevicius, I. MacDonald, M. Shkunov, D. Sparrow, S. Tierney, R. Wagner, W. Zhang, M. L. Chabynyc, R. J. Kline, M. D. McGehee, M. F. Toney, *Nat. Mater.* **2006**, *5*, 328.
- [14] a) F. Dierschke, A. C. Grimdale, K. Müllen, *Synthesis* **2003**, *16*, 2470; b) X. Pan, S. Liu, H. S. O. Chan, S.-C. Ng, *Macromolecules* **2005**, *38*, 7629.
- [15] M. J. Marsella, Z.-Q. Wang, R. J. Reid, K. Yoon, *Org. Lett.* **2001**, *3*, 885.